

RESEARCH ARTICLE

Enterovirus 71 Infection Causes Severe Pulmonary Lesions in Gerbils, *Meriones unguiculatus*, Which Can Be Prevented by Passive Immunization with Specific Antisera

Fang Xu¹✉, Ping-Ping Yao¹✉, Yong Xia¹, Lei Qian¹, Zhang-Nv Yang¹, Rong-Hui Xie¹, Yi-Sheng Sun¹, Hang-Jing Lu¹, Zi-Ping Miao¹, Chan Li¹, Xiao Li², Wei-Feng Liang³, Xiao-Xiao Huang⁴, Shi-Chang Xia¹, Zhi-Ping Chen^{1*}, Jian-Min Jiang¹, Yan-Jun Zhang¹, Ling-Ling Mei¹, She-Lan Liu¹, Hua Gu¹, Zhi-Yao Xu⁵, Xiao-Fei Fu⁶, Zhi-Yong Zhu^{1*}

1 Key Lab of Vaccine against Hemorrhagic Fever with Renal Syndrome, Zhejiang Province Center for Disease Prevention and Control, Hangzhou, China, **2** Department of Pathology, First Municipal Hospital of Hangzhou, Hangzhou, China, **3** The First Affiliated Hospital, Zhejiang University, Hangzhou, China, **4** Hangzhou Sixth People's Hospital, Hangzhou, China, **5** Wenzhou Medical University, Wenzhou, China, **6** Jiaying Center for Disease Control and Prevention, Jiaying, China

✉ These authors contributed equally to this work.

* hanpingzhu@aliyun.com (HPZ); zhpchen@cdc.zj.cn (ZPC)



OPEN ACCESS

Citation: Xu F, Yao P-P, Xia Y, Qian L, Yang Z-N, Xie R-H, et al. (2015) Enterovirus 71 Infection Causes Severe Pulmonary Lesions in Gerbils, *Meriones unguiculatus*, Which Can Be Prevented by Passive Immunization with Specific Antisera. PLoS ONE 10(3): e0119173. doi:10.1371/journal.pone.0119173

Academic Editor: Jie Sun, Indiana University, UNITED STATES

Received: June 23, 2014

Accepted: January 10, 2015

Published: March 13, 2015

Copyright: © 2015 Xu et al. This is an open access article distributed under the terms of the [Creative Commons Attribution License](https://creativecommons.org/licenses/by/4.0/), which permits unrestricted use, distribution, and reproduction in any medium, provided the original author and source are credited.

Data Availability Statement: All relevant data are within the paper and its Supporting Information files.

Funding: The work was granted by Natural Science Foundation of Zhejiang Province (Y3100701) and the Medical and Technological Project of Zhejiang Province (2010KYB027). The funders had no role in study design, data collection and analysis, decision to publish, or preparation of the manuscript.

Competing Interests: The authors have declared that no competing interests exist.

Abstract

Neurogenic pulmonary edema caused by severe brainstem encephalitis is the leading cause of death in young children infected by Enterovirus 71 (EV71). However, no pulmonary lesions have been found in EV71-infected transgenic or non-transgenic mouse models. Development of a suitable animal model is important for studying EV71 pathogenesis and assessing effect of therapeutic approaches. We had found neurological disorders in EV71-induced young gerbils previously. Here, we report severe pulmonary lesions characterized with pulmonary congestion and hemorrhage in a gerbil model for EV71 infection. In the EV71-infected gerbils, six 21-day-old or younger gerbils presented with a sudden onset of symptoms and rapid illness progression after inoculation with $1 \times 10^{5.5}$ TCID₅₀ of EV71 via intraperitoneal (IP) or intramuscular (IM) route. Respiratory symptoms were observed along with interstitial pneumonia, pulmonary congestion and extensive lung hemorrhage could be detected in the lung tissues by histopathological examination. EV71 viral titer was found to be peak at late stages of infection. EV71-induced pulmonary lesions, together with severe neurological disorders were also observed in gerbils, accurately mimicking the disease process in EV71-infected patients. Passive transfer with immune sera from EV71 infected adult gerbils with a neutralizing antibody (GMT=89) prevented severe pulmonary lesion formation after lethal EV71 challenge. These results establish this gerbil model as a useful platform for studying the pathogenesis of EV71-induced pulmonary lesions, immunotherapy and antiviral drugs.

Introduction

Enterovirus 71 (EV71), a member of the genus *Enterovirus* within the family *Picornavirus*, affects mostly infants and young children [1–3]. EV71 infection usually leads to hand, foot, and mouth disease (HFMD) and sometimes causes severe neurological manifestations including aseptic meningitis, encephalitis, acute flaccid paralysis, and pulmonary edema, with the percentage of pulmonary edema or hemorrhage considerably high in the fatal cases [4,5]. EV71-infection, responsible for severe nervous system damage and death, is now considered the most important neurotropic enterovirus following the eradication of poliomyelitis [6].

In 2010 alone, at least 1.7 million HFMD cases were reported with 905 deaths [7]. Between 2008 and 2012, there were 7.2 million probable HFMD cases and a potential 2,457 EV71-related deaths reported to Chinese Center for Disease Control and Prevention [8]. Although EV71 outbreaks have occurred sporadically in several geographies, several large outbreaks have occurred in Asia-Pacific region including mainland China [9–11], Taiwan [4], South Korea [12], Japan [13], Singapore [14], Malaysia [15], Thailand, and Vietnam [16]. The 1998 Taiwanese outbreak resulted in 65 HFMD deaths of EV71-infected children, mainly due to pulmonary edema or hemorrhage [4]. EV71 was confirmed as the major pathogen in the 2008 Chinese outbreak that resulted in 4.89 million HFMD cases and 126 deaths [10].

Children infected with EV71 tend to have a faster disease progression, higher fever and a higher incidence of limb movement disorder, coma, neurological damage, neurogenic pulmonary edema and death compared to other enterovirus strains [17]. However, the pathogenesis of EV71 infection is not clearly elucidated. Though several mouse species have been used to study EV71 infection and pathogenesis (BALB/c, ICR, NOD/SCID, AG129, and transgenic strains), no models were successful in inducing pulmonary edema [18–25]. In previous studies, we demonstrated that gerbils infected with EV71 developed symptoms related to neurological lesions including hind limb paralysis, slowness, ataxia and lethargy [26]. In this report, we found that gerbils aged 7 to 21 days infected with EV71 by intraperitoneal (IP) or intramuscular (IM) routes and exhibited severe pulmonary lesions. We also demonstrated that EV71-induced pulmonary lesions could be prevented by passive transfer of specific EV71-antisera after lethal EV71 challenge. Therefore, the gerbil EV71 model may serve as a useful animal model for studying the pathogenesis of EV71-mediated pulmonary disease and assessing novel therapeutic interventions.

Materials and Methods

Virus

The EV71 strain used in this study (58301, genotype C4) was isolated from a vesicle swab obtained from a 12-month-old child with mild HFMD in 2008 in Hangzhou, China [26]. The child's parents provided written informed consent for the scientific use of the sample, and Hangzhou Sixth People's Hospital Ethics Committee approved the project. EV71 was grown in the Vero cells and passaged no more than five generations before use. EV71 was stored in aliquots at -70°C in modified Eagle's medium (MEM) supplemented with 10% fetal bovine serum (FBS). Virus titer was $1 \times 10^{7.0}$ tissue culture infection dose (TCID_{50}) determined using Vero cells according to the Reed—Muench method [27].

Animals and EV71 infection

Gerbils were purchased from the Animal Center of Zhejiang Academy of Medical Sciences, Hangzhou, China. The animals were housed under standard laboratory conditions (relative humidity $50 \pm 5\%$, room temperature $24 \pm 1^{\circ}\text{C}$, and 12 hrs light dark cycle) in Plexiglas cages

(Techniplast, Italy; 1291H). The animals were fed with a standard diet and had unlimited access to water. All animal experimental procedures were performed following the Regulations for the Administration of Affairs Concerning Experimental Animals of the People's Republic of China, and were approved by Institutional Animal Care and Use Committee of Zhejiang Provincial Center for Disease Control and Prevention.

Gerbils were inoculated with EV71 via either an IP, IM, or intracranial (IC) route, and clinical scores were defined as following: 0, healthy; 1, ruffled hair, hunchbacked or reduced mobility; 2, limb weakness; 3, paralysis in one limb; 4, paralysis in both limbs or deep lethargy; 5, death. When infected-gerbils showed grade 4 symptoms, gerbils were humanely sacrificed. While gerbils were most susceptible to EV71 infection via IC, this usually led to mechanical injury and unnatural death (data not shown). While IP and IM routes had similar infection rates in gerbils, the IP route was chosen as the primary inoculation route for its convenience.

Four sets of animal experiments were performed. In the first study, gerbils were inoculated via the IP route with $1 \times 10^{5.5}$ TCID₅₀ of EV71 at 7, 14, 21, 28 and 35 days ($n = 6$ for each age group). In the second study, 21-day-old gerbils were inoculated with $1 \times 10^{3.5}$ or $1 \times 10^{5.5}$ TCID₅₀ of EV71 via the IP route ($n = 8$ for each dose group). In the third study, 21-day-old gerbils were inoculated with $1 \times 10^{5.5}$ TCID₅₀ of EV71 via IP, IM or oral (OL) routes respectively. Eight gerbils were used for each different infection routes. These gerbils were observed daily for 20 days after inoculation. When infected-gerbils showed grade 4 symptoms, gerbils were euthanized and tissues were collected for histological examination. In the fourth study, three 50-day-old gerbils were administered EV71 via the IP route with $1 \times 10^{5.5}$ TCID₅₀ of EV71, blood samples were collected at 0, 7, 14, 21, 28 and 35 days post infection (p.i.) for EV71 neutralizing antibody analysis.

Lung virus titer of infected gerbils

Lung tissues were collected after signs of lethargy or 2 hind limb paralysis appeared in EV71-infected gerbils at the age of 7, 14, 21, 28, and 35 d. After perfusion with 0.02 M PBS (pH = 7.2), lung tissue samples were aseptically removed, weighed, and stored at -70°C . The tissue samples were homogenized in PBS to generate a 10% solution followed by freezing and thawing three times. The tissue suspension was centrifuged at $1000 \times g$ for 5 min at 4°C to remove tissue debris. The supernatants were serially diluted in MEM, and 100 μL of each dilution were placed onto monolayer of Vero cells in 96-well plates for virus titration. Following 4-day incubation at 37°C , the plates were scored for cytopathic effects (CPE) positive wells microscopically and the TCID₅₀ was determined by the highest diluted titers and expressed as $\log \text{TCID}_{50} / \text{g}$ of tissue.

Histological examination

Lung tissues from the gerbils exhibiting clinical symptoms (approximately 4–5 day p.i.) were fixed in 10% formalin in PBS for 48 h and embedded in paraffin. The paraffin-embedded tissue sections were mounted on poly-L-lysine-coated slides, and stained with hematoxylin and eosin for morphological examination as described previously [26].

Quantitative RT-PCR

Tissues from gerbils were homogenized and total RNA was prepared using the RNeasy Mini kit (Qiagen, USA) according to the manufacturer's instructions. The extracted RNA was analyzed for the viral load using the TaqMan quantitative RT-PCR for amplification of the EV71 VP1 gene as described previously [26]. Each assay was performed in triplicate. The standard curve was created by 10-fold serial dilutions of stock EV71 ($1 \times 10^{7.0}$ TCID₅₀/mL).

Detection of antibodies against EV71

Blood samples were collected from 50-day-old gerbils on days 0, 5, 7, 14, 21, 28, and 35 post-EV71 inoculation. EV71 neutralizing antibodies were analyzed using a standard protocol. Briefly, two-fold dilutions of heat-inactivated sera were mixed with 50 μL EV71-containing solution at a dose of $1 \times 10^{2.0}$ TCID₅₀ per well in a 96-well plate, and incubated for 2 h at 37°C. After incubation, mixtures were added onto monolayer of Vero cells and the cells were inspected daily for CPE up to 4 d. Neutralizing antibody titers were determined as the highest dilution of serum that inhibited virus growth. Fluorescent antibodies to EV71 were identified using an indirect immunofluorescence assay (IFA). Briefly, 10 μL of two-fold serially diluted sera were applied to each well of the slide containing EV71-infected Vero cells fixed in acetone and incubated for 30 min at 37°C. Following washing in 1X PBS three times for 10 min, slides were combined with 10 μL fluorescein isothiocyanate (FITC)-labeled anti-mouse IgG (Sigma) at 37°C for 30 min. The slides were washed as before, covered with cover slips, and fluorescence was examined under a fluorescent microscope (Leica DMI 4000B, Leica Microsystems, Wetzlar, Germany).

Passive immunization

Adult gerbils were immunized with formalin-inactivated EV71 and boosted 1 week later [26]. Serum samples were collected from the immunized gerbils 1 week post-boosting dose and following the same time course for the mock-immune gerbils. Heat-inactivated (56°C for 30 min) sera were tested for neutralizing antibodies against EV71 at dilutions up to 1:256. The 21-day-old treatment group was passively immunized by IP with 100 μL immune sera and challenged with IP injection 1 h later with $100 \times \text{HD}_{50}$ (humane endpoint) of EV71. A second dose of immune sera was administered 24 h post-challenge. Twenty-one-day-old gerbils ($n = 5$) from control groups were given mock-immune sera. Gerbils were monitored for 20 days post-challenge for clinical symptoms.

Statistical analysis

All statistical analyses were done with GraphPad Prism, version 5.0 (GraphPad 4 Software, San Diego, CA). The survival rates of gerbils infected with EV71 were analyzed by log-rank analysis. Clinical scores were analyzed using the Wilcoxon test. Viral copies in tissues after EV71 infection were expressed as mean \pm SD and analyzed with a Student's *t* test by SPSS software. A *P* value less than or equal to 0.05 was considered statistically significant.

Results

Clinical symptoms after EV71 infection

In order to examine the susceptibility of gerbils at different ages to EV71 infection, three groups of gerbils at the age of 7, 14 and 21 days were IP inoculated with $1 \times 10^{5.5}$ TCID₅₀ of EV71 ($n = 6$ for each age groups). All gerbils presented with a sudden onset of symptoms at 3–4 days post-inoculation. In addition, all gerbils showed disease signs including progressing weakness, one or two hind limb paralysis and deep lethargy. Illness progressed rapidly and usually caused death within 12 hours of onset. Ten gerbils (two in 7 days, four in 14 days and four in 21 days of age) also had respiratory system symptoms including tachypnea, respiratory distress, apnea, or rhythm changes. Clinical signs between the three age groups were not different, with the only variation of the time from EV71 inoculation to disease onset. The average time of disease onset and death was 3 and 3.7 p.i., respectively, for gerbils in the 7-day-old group. For gerbils in the 14-day-old or 21-day-old groups, the average time of disease onset was 4–5 days and death

occurred within 6–12 h after clinical signs occurred. In the 28-day-old group, two of out six gerbils began to exhibit hind limb weakness and paralysis five days post-IP inoculated with $1 \times 10^{5.5}$ TCID₅₀ of EV71 and died two days later. Four gerbils survived and one experienced hind limb paralysis. There was no mortality in the 35-day-old group with only two gerbils presenting with hind limb paralysis (Fig. 1A, S1–S5 Tables). These data demonstrated that gerbils aged 7–21 days were most sensitive to the EV71 infection.

Based on the above clinical findings, we further investigated the course of EV71 infection and disease progression in 21-day-old gerbils by IP inoculation at lower EV71 doses ($1 \times 10^{3.5}$ TCID₅₀). Gerbils infected at these lower doses developed clinical signs later than higher dose group ($1 \times 10^{5.5}$ TCID₅₀), with the average time from infection to symptoms onset equaling seven days. Furthermore, three of eight gerbils were asymptomatic after lower dose infection, while two were positive for anti-EV71 antibodies. Finally, the incidence of death was 62.5% (5/8) versus 100% in high titer infected animals (Fig. 1B, S6 Table). These data indicate that disease progress and death rate are dose dependent, which may relate to high virus replication level in the targeted organs of gerbils infected with higher doses of EV71.

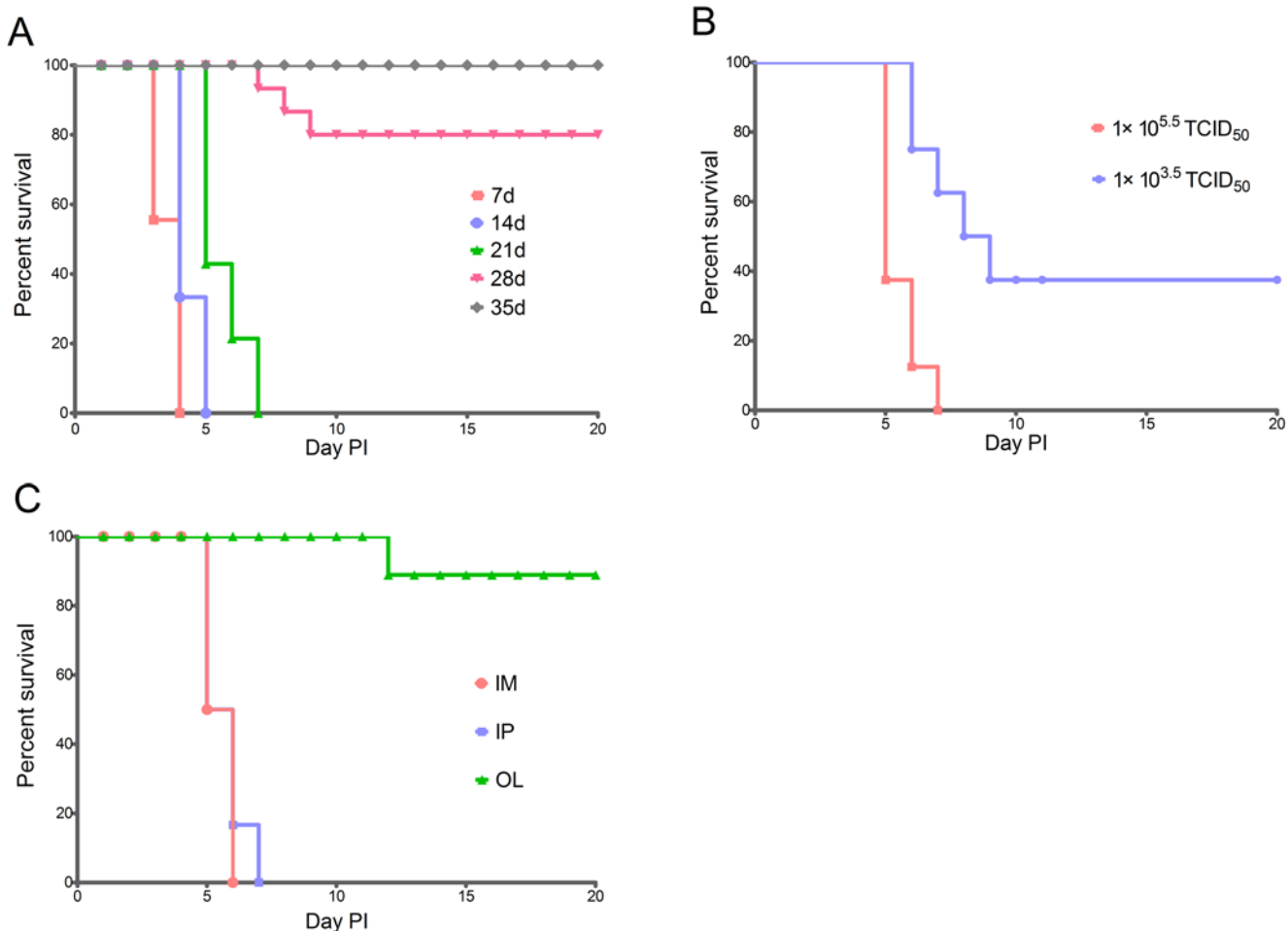


Fig 1. Survival rates of gerbils infected with EV71. (A) Gerbils (7, 14, 21, 28, and 35 d old) were inoculated IP with $1 \times 10^{5.5}$ TCID₅₀ of EV71 (n = 6 for each age group). (B) 21-day-old gerbils were inoculated with $1 \times 10^{3.5}$ or $1 \times 10^{5.5}$ TCID₅₀ of EV71 via IP (n = 8 for each dose group). (C) 21-day-old gerbils were inoculated with $1 \times 10^{5.5}$ TCID₅₀ of EV71 via IP, IM or OL respectively.

doi:10.1371/journal.pone.0119173.g001

To analyze the susceptibility of gerbils to EV71 by different injection routes, 24 21-day-old gerbils were inoculated with EV71 ($1 \times 10^{5.5}$ TCID₅₀) by IM, IP, or OL route ($n = 8$ for each route). Disease onset was similar between IM and IP routes (4–5 day p.i), and all gerbils died by 5–7 days after inoculation. In contrast OL administration of EV71 led to a time of disease onset of 10 days p.i. and only one gerbil died during the experimental period (Fig. 1C, S7 Table). The HD₅₀ for IM and IP inoculation were $1 \times 10^{3.0}$ TCID₅₀ and $1 \times 10^{2.64}$ TCID₅₀, respectively.

Histopathological observations in lung tissues

For gerbils, the spinal cord, brainstem and skeletal muscle are the target organs of EV71-infection [26]. Neuronal degeneration, neuronal loss and neuronophagia in central nervous system (CNS) and necrotizing myositis in skeletal muscle were observed in the infected gerbils [26]. In this study, severe damage in lung tissues were also found in infected gerbils. Lung tissue from EV71-infected gerbils was observed to be more dark red than that from normal gerbils (Fig. 2). Microscopically, lung tissue from healthy gerbils showed normal alveoli, alveolar septa, and lining epithelium (Fig. 3A). In contrast, lung tissues of EV71-infected gerbils revealed diffused lesions and dysfunctions with varying degrees of severity. Pulmonary interstitial inflammatory and alveolar septum broadening was observed in all EV71-infected gerbils after EV71 inoculation at both high IP dosing in all three age groups ($1 \times 10^{5.5}$ TCID₅₀; 7 d, 14 d, 21d) (Fig. 3B). A thickened alveolar septum resulting from inflammation, scarring, or extra fluid (edema) was the main histological feature (Fig. 3C). Occasionally, lung tissue or alveolar space contained liquid instead of gas (Fig. 3D) and focal alveolar hemorrhaging was noted (Fig. 3E). One third of infected gerbils (6/18) developed focal alveolar consolidation and many neutrophilic infiltrates were found within the alveolar spaces (Fig. 3F). In addition, another one third developed diffuse alveolar hemorrhaging and lumina of alveoli with bronchioles minority filled with edema fluid (Fig. 3G). There was no obvious difference in histopathology in infected gerbils among the three age groups (Table 1). These data indicated gerbils aged from 7–21 days exhibited an age-independent response to lung tissue damage and death rate although the time to disease onset was different in each. Both 28-day-old and 35-day-old gerbils showed only pulmonary interstitial thickening, with no extensive pulmonary hemorrhaging observed (data not shown).

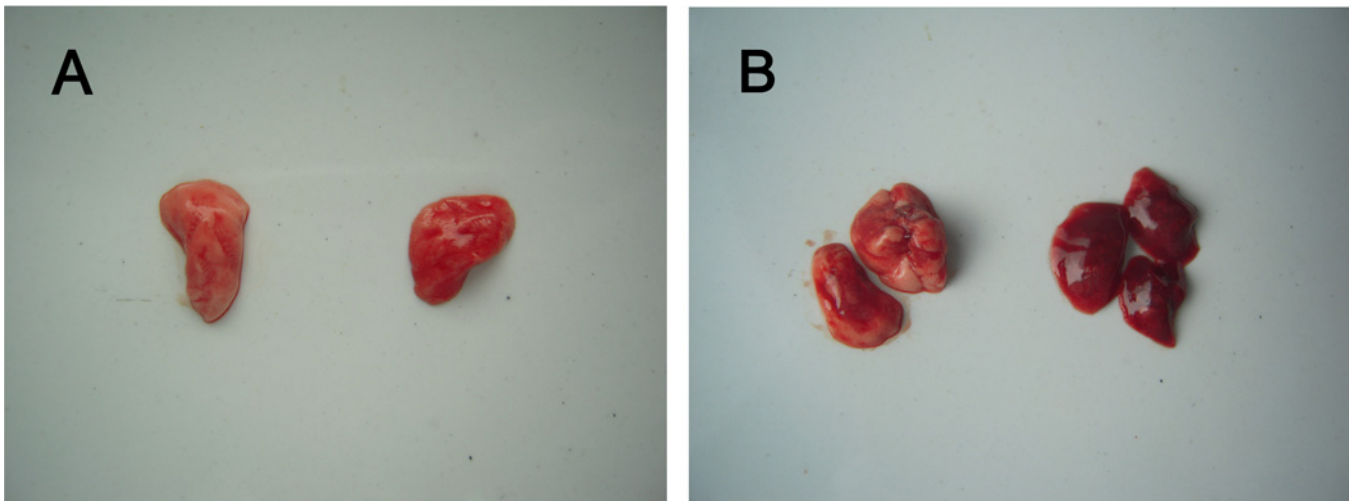


Fig 2. Macroscopic pathological lung changes in EV71-infected 21-day-old gerbils following $1 \times 10^{5.5}$ TCID₅₀ inoculation by IP route. Pictures correspond to the lung tissues from healthy or EV71-infected gerbils. Normal lung of a healthy gerbil (A, left; B, left), markedly red and congestion, extensive hemorrhage (A, right; B, right) in the lung were shown in EV71-infected gerbils.

doi:10.1371/journal.pone.0119173.g002

Gerbils infected with different doses of EV71 showed different pathology changes. In the high dose groups ($1 \times 10^{5.5}$ TCID₅₀), as much as 90% of the lung tissue had been destroyed, with multiple foci of interstitial inflammatory cell infiltration, alveolar septum broadening, alveolar consolidation and local pulmonary hemorrhage observed (Fig. 3H). The main lesion characteristic was pulmonary interstitial inflammation. The most severe lung lesion was extensive pulmonary hemorrhaging in 37.5% (3/8) of EV71-infected gerbils (Fig. 3I). In the low dose groups ($1 \times 10^{3.5}$ TCID₅₀), only 10–20% of the lung tissue had histological changes and no extensive pulmonary hemorrhaging was observed (Table 2). There were no obvious differences in histological examination between the IP and IM injected route. Evidence of very few areas of pulmonary interstitial thickening and alveolar septum broadening was found in the OL route groups. No local or extensive pulmonary hemorrhage was found (Table 3).

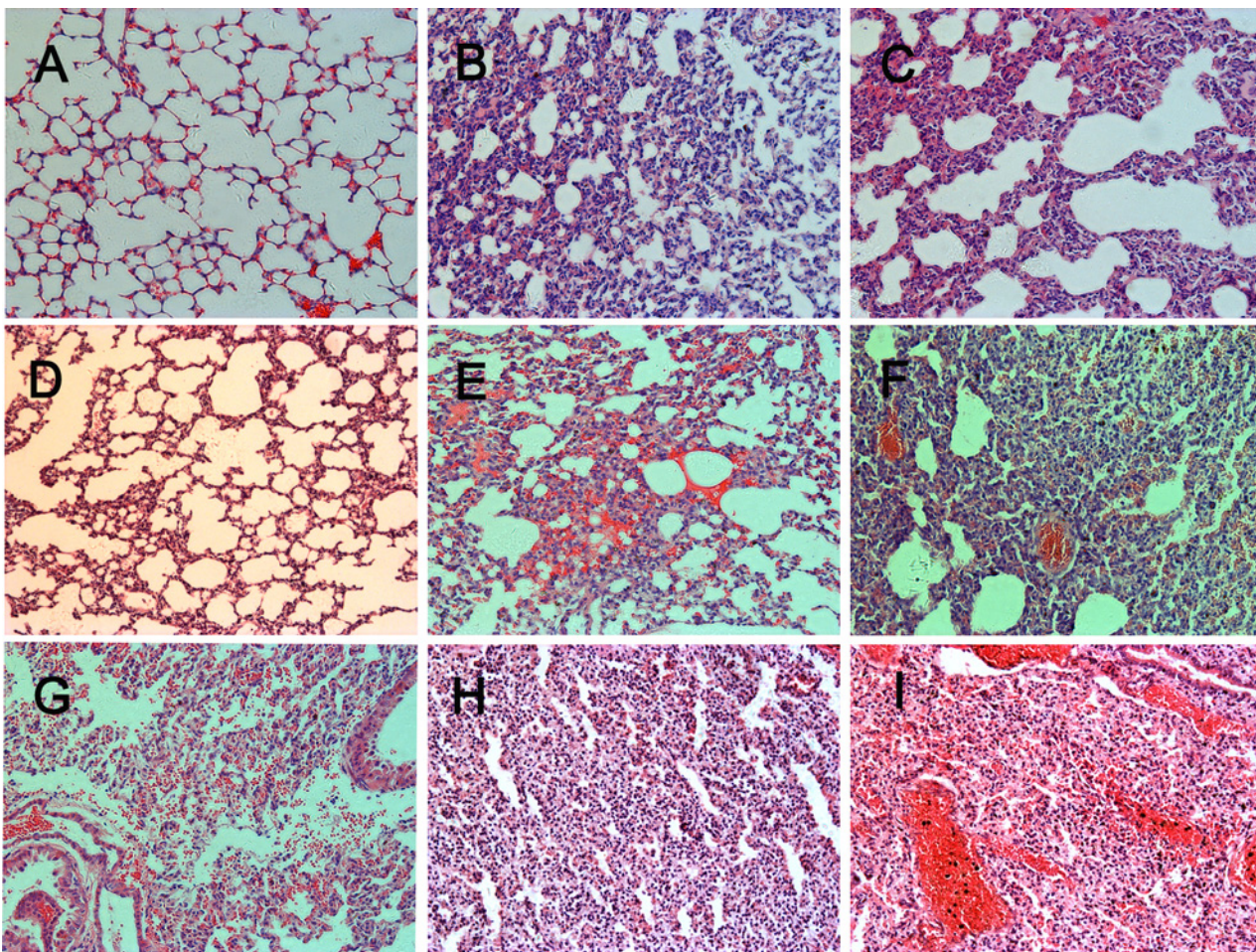


Fig 3. Serial pathological changes in lung tissues of gerbils infected with $1 \times 10^{5.5}$ TCID₅₀ EV71 by IP route. (A) Normal gerbil lung tissues. Typical lesions included multiple foci of pulmonary interstitial inflammatory (B) and alveolar septum broadening (C) was seen in lung at the age of 7–21 days of EV71-infected gerbils. Some fluid could be seen in alveolar space (D) and focal alveolar hemorrhage were noted (E). Local pulmonary consolidation (F) and the lumina of alveoli and bronchioles were filled with edema fluid and red cells (G). Extensive alveolar consolidation, pulmonary interstitial inflammatory cell infiltration (H), or extensive pulmonary hemorrhage and alveolar spaces filled with mononuclear and neutrophilic infiltration (I) were shown at the end stage of EV71-infection. Hematoxylin and eosin stain; magnification: A-I, 200x.

doi:10.1371/journal.pone.0119173.g003

Table 1. Lung pathology following EV71 infection.

Pathological findings	7 d (n = 6)		14 d (n = 6)		21 d (n = 6)	
	n	%	n	%	n	%
Pulmonary interstitial inflammatory cell infiltration	6	100.0	6	100.0	6	100.0
Alveolar septum broadening	6	100.0	6	100.0	5	83.3
Local alveolar consolidation	2	33.3	1	16.7	3	50.0
Interstitial pulmonary congestion	6	100.0	6	100.0	5	83.3
Extensive pulmonary hemorrhage	2	33.3	1	16.7	3	50.0
Extensive alveolar consolidation	4	66.7	3	50.0	1	16.7
Oedema fluid in alveolar or bronchus	2	33.3	2	33.3	5	83.3

doi:10.1371/journal.pone.0119173.t001

Virus replication in organs of infected gerbils

We examined the viral replication in gerbils infected with a dose of $1 \times 10^{5.5}$ TCID₅₀ by IP route in animals of five different ages. Virus isolated from the lung was detectable as early as one day p.i. with viral titers almost the same for 7–21 day-old gerbils. Further, this number was lower for 28–35 day old gerbils. Thereafter, virus titers increased gradually and reached a peak at the end of stage of EV71-infection in five age groups (Fig. 4A). In other tissues, such as liver, kidney, pancreas, stomach and spleen, virus replicated to the same level as that in lung tissues. The peak virus titers in the lung ($1 \times 10^{5.75}$ TCID₅₀) were lower than that in the spinal cord, brainstem or skeletal muscle, the location of the highest observed virus titer $1 \times 10^{7.5-8.25}$ TCID₅₀ (Fig. 4B). Therefore, lung tissue was not the major target organ of EV71 infection in young gerbils. These data indicate that EV71 is a CNS- and muscle-tropic virus.

Peak virus titer was observed approximately one to two days later when infected with lower doses of EV71 ($1 \times 10^{3.5}$ TCID₅₀). Further, the peak titer only reached $1 \times 10^{3.25}$ TCID₅₀; approximately two logs lower than those infected with high doses (Fig. 4C). In three asymptomatic gerbils infected with lower doses of EV71, no virus was detected in the lung tissues of two gerbils. These data suggest disease progression is dose dependent.

EV71-specific antibodies in gerbils

Considering 7, 14, and 21 day-old gerbils infected via the IP route, all gerbils died before antibodies could be detected, we used 50-day-old gerbils for antibody detection. Eight gerbils were

Table 2. The pathological types of lungs in EV71-infected gerbils with different virus doses.

Pathological findings	Virus titer $1 \times 10^{5.5}$ (n = 8)		Virus titer $1 \times 10^{3.5}$ (n = 8)	
	n	%	n	%
Pulmonary interstitial inflammatory cell infiltration	8	100.0	6	75.0
Alveolar septum broadening	8	100.0	6	75.0
Local alveolar consolidation	5	62.5	2	25.0
Interstitial pulmonary congestion	5	62.5	4	50.0
Extensive pulmonary hemorrhage	3	37.5	0	0
Extensive alveolar consolidation	1	12.5	0	0
Oedema fluid in alveolar or bronchus	5	62.5	5	62.5

21-day-old gerbils were inoculated EV71 by IP route.

doi:10.1371/journal.pone.0119173.t002

Table 3. The pathological types of lungs in EV71-infected gerbils via different routes.

Pathological findings	IP (n = 8)		IM (n = 8)		OL (n = 8)	
	n	%	n	%	n	%
Pulmonary interstitial inflammatory cell infiltration	8	100.0	8	100.0	4	50.0
Alveolar septum broadening	8	100.0	8	100.0	4	50.0
Local alveolar consolidation	3	37.5	5	62.5	1	12.5
Interstitial pulmonary congestion	7	87.5	8	100.0	3	37.5
Extensive pulmonary hemorrhage	3	37.5	4	50	0	0
Extensive alveolar consolidation	4	50.0	3	37.5	0	0
Oedema fluid in alveolar or bronchus	7	87.5	7	87.5	3	37.5

21-day-old gerbils were inoculated with $1 \times 10^{5.5}$ TCID₅₀ EV71.

doi:10.1371/journal.pone.0119173.t003

inoculated via the IP route with $1 \times 10^{5.5}$ TCID₅₀ EV71, and neutralizing antibodies were detected as early as day five days p.i. and peaked at 28 days p.i. at a ratio of 1:75.39 (Fig. 5).

Protection against lung lesions in gerbils by passive immunization

Passive immunization was used to evaluate the effects of humoral immunity in protecting against EV71 lethal challenge. Gerbils were passively immunized with neutralizing antibodies (GMT = 89; 100 µL/gerbil). Two doses fully protected gerbils from EV71 lethal challenge. In

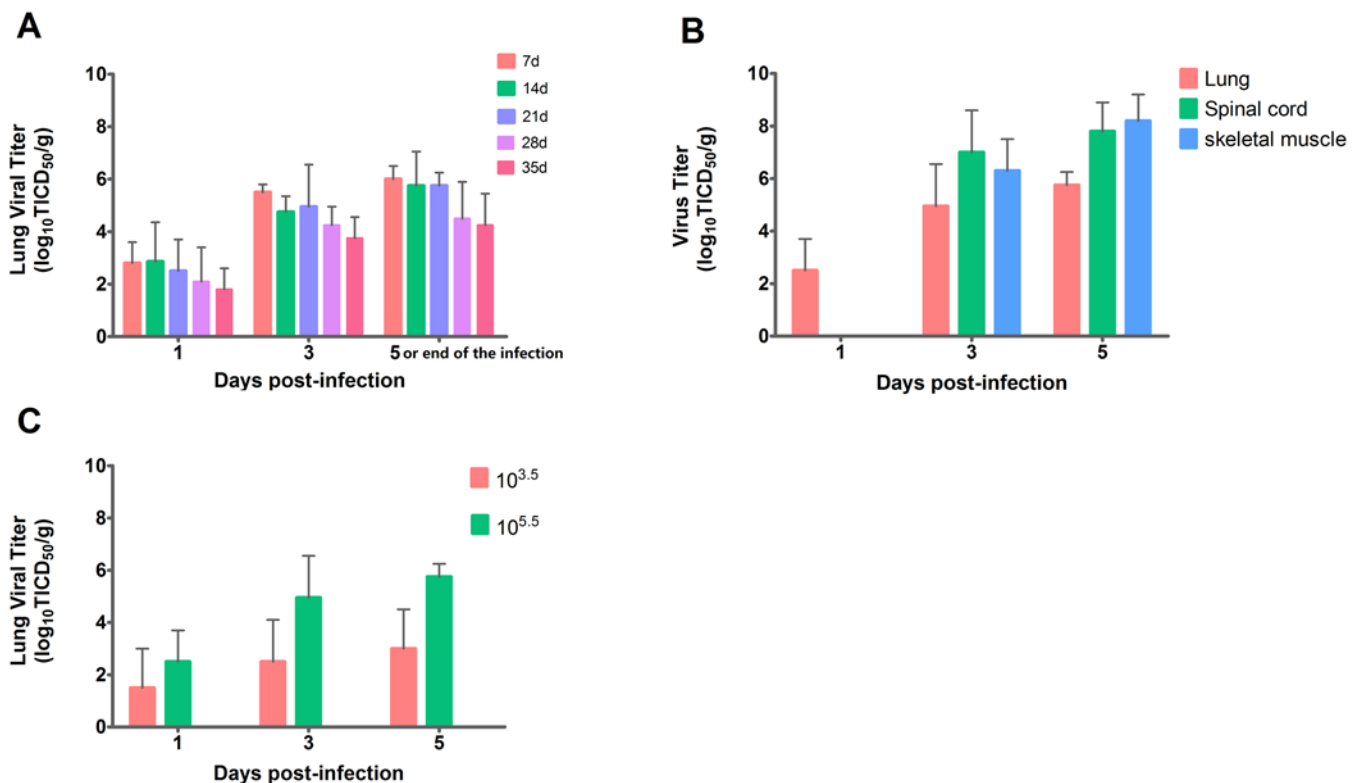


Fig 4. Virus replication in lung and other tissues of EV71-infected gerbils. (A) gerbils (7, 14, 21, 28, 35 d old) were inoculated IP with $1 \times 10^{5.5}$ TCID₅₀ of EV71 (n = 6 for each age groups). (B) Virus titer in various tissues was determined in 21-day-old gerbils inoculated with $1 \times 10^{5.5}$ TCID₅₀ of EV71 via IP route (n = 8 for each dose group). (C) 21-day-old gerbils were inoculated with $1 \times 10^{3.5}$ or $1 \times 10^{5.5}$ TCID₅₀ of EV71 via IP.

doi:10.1371/journal.pone.0119173.g004

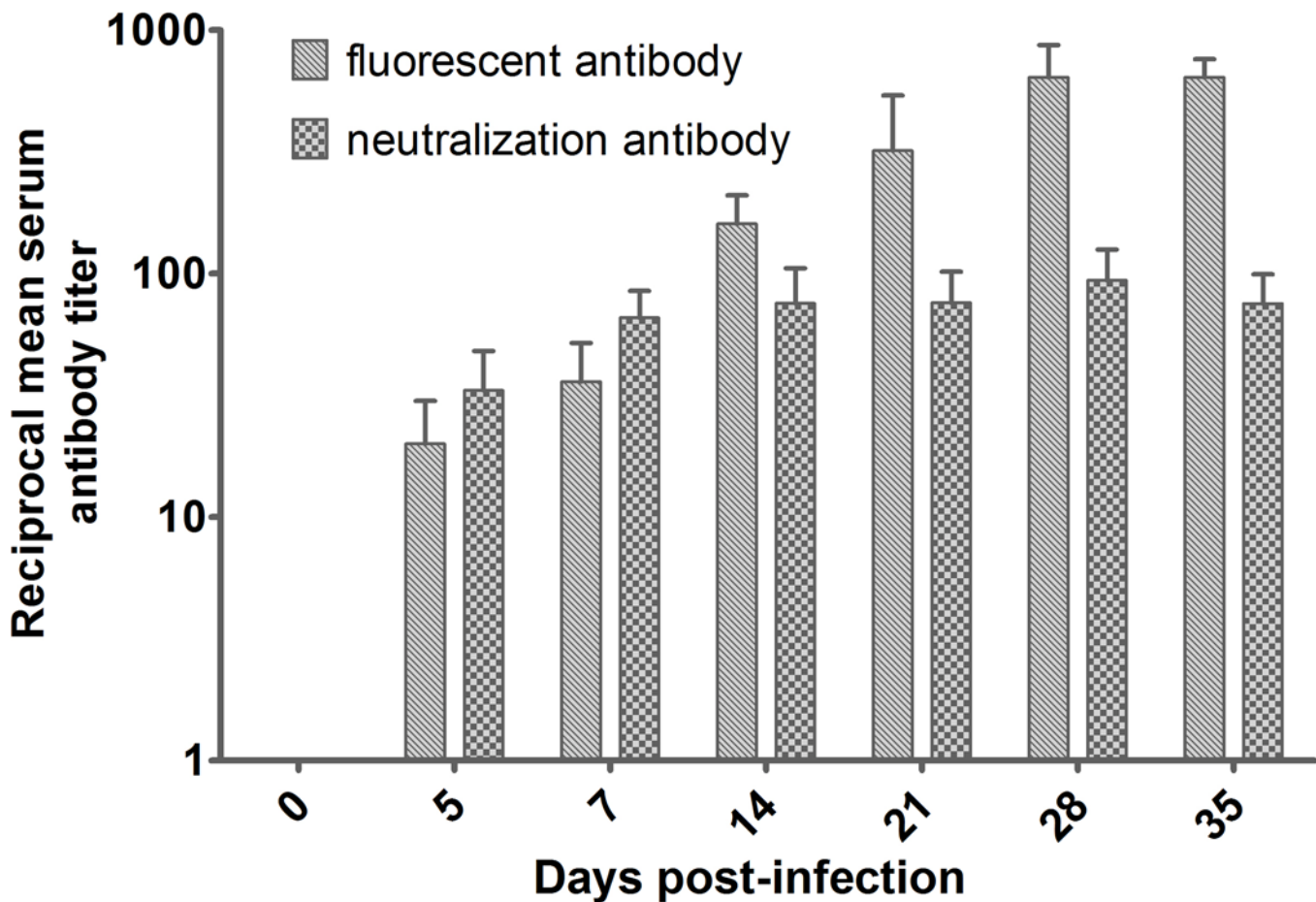


Fig 5. The reciprocal neutralizing antibody and fluorescent antibody titers of EV71-specific serum in infected gerbils following IP inoculation with $1 \times 10^{5.5}$ TCID₅₀ EV71. The solid line indicates mean antibody titer from three gerbils per group on a logarithmic scale for each day. Error bars represent the standard deviation.

doi:10.1371/journal.pone.0119173.g005

contrast, mock-immunized gerbils developed hind limb paralysis and were dead at 5–6 days post-challenge (Fig. 6). Histological examination indicated gerbils that received the anti-EV71 antibodies had intact lung structures without detected EV71-induced lesions and no virus copies were detected in lungs by real-time RT-PCR. Mock-immunized gerbils revealed severe lung pathology including pulmonary interstitial inflammatory infiltration and alveolar septum broadening (Fig. 7). These results demonstrate passively acquired protection against EV71-induced lung lesions in the gerbil model is mediated by specific antisera containing neutralizing antibodies to EV71.

Discussion

This study describes a promising animal model for the study of EV71 infection. Specifically, this experimental gerbil model is the first to demonstrate severe pulmonary lesions upon infection with this virus. We examined histopathological changes and virus replication in lung tissues of EV71-infected gerbils. Our results indicated that gerbils were susceptible to EV71 infection and the resulting severe pulmonary lesions when inoculated via IM or IP routes within the suckling periods (first 21 days of life). Symptoms such as interstitial pneumonia, pulmonary congestion and extensive lung hemorrhaging correlated with virus replication in the host

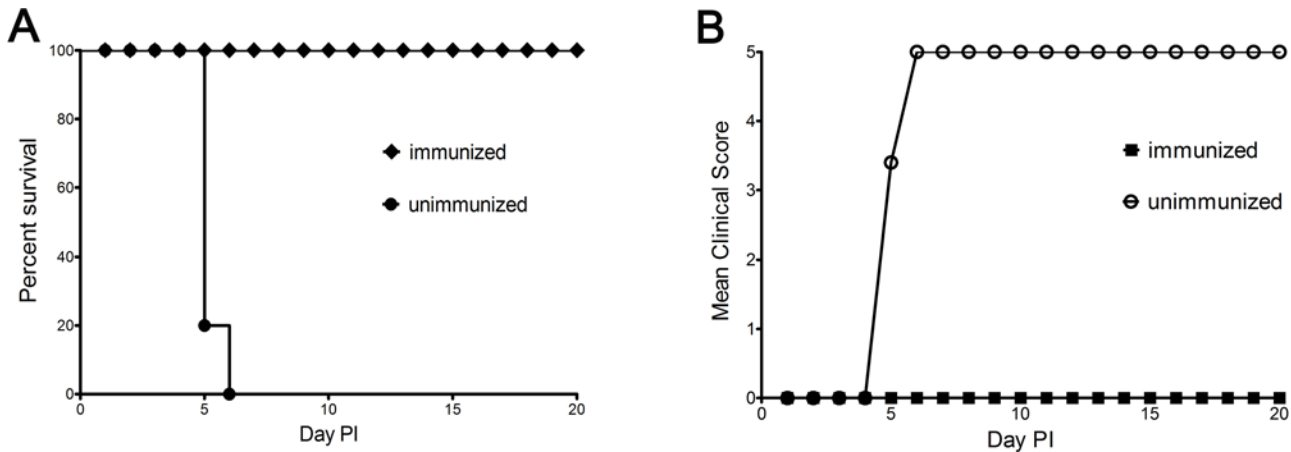


Fig 6. Survival and clinical score of immunized gerbils after IP challenge with humane doses of EV71 (100xHD₅₀). Experiment groups (n = 5) were immunized with anti-EV71 antisera at 21-days-old as described in Materials and Methods. The control groups (n = 5) were given normal saline. All gerbils were challenged by the IP route with lethal doses of EV71 at post-immunization. The survival rates and clinical scores were monitored daily after challenge. *P* = 0.001.

doi:10.1371/journal.pone.0119173.g006

animal lungs. Importantly, we demonstrated a protective role for passive antibody treatment in preventing disease in the gerbil model.

Many animal models have been used to study EV71 infection. Fourteen-day-old ICR mice, human SCARB2 transgenic mice and 14-day-old AG129 mice lacking IFN- α/β and IFN- γ receptor could mimic some neurologic complications typically observed in human EV71 infection [20,28–30]. The non-human primate model is much more similar to humans, however, only 10% of EV71-infected cynomolgus monkeys developed neurological disease[31]. Therefore, pulmonary lesion had not been reflected in these animal models which limits the applicability for understanding EV71 disease mechanisms [32]. In this study, we found gerbils developed unique severe pulmonary lesions after EV71 infection via IP or IM routes and the disease progressed rapidly with death occurring within 12 hours of first observing symptoms.

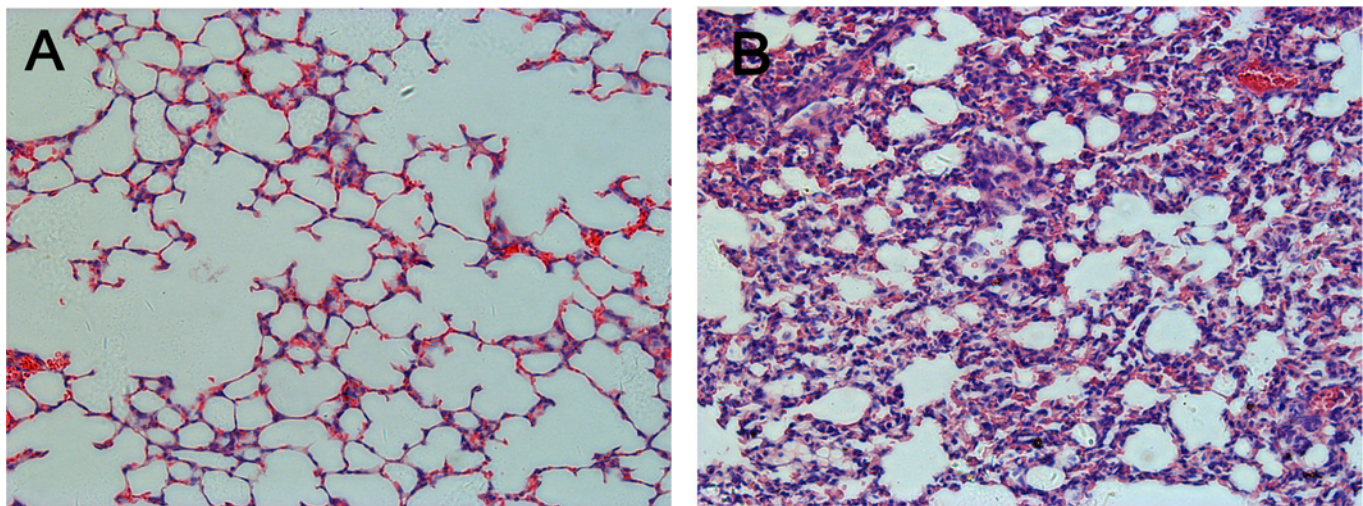


Fig 7. Histological examinations of lung in 21-day-old gerbils challenged with humane doses 100xHD₅₀ EV71. (A) Gerbils receiving EV71-antisera revealed no evidence of inflammation and structures of the lungs appeared intact. (B) Gerbils receiving the mock sera, lung structures were damaged and multiple foci of pulmonary interstitial inflammatory were observed. Hematoxylin and eosin stain; magnification: A, B 200x.

doi:10.1371/journal.pone.0119173.g007

Severe histopathological changes, including interstitial pneumonia, pulmonary lesions and extensive hemorrhaging, were observed in the lung tissue. We hypothesized that the presence of pulmonary lesions or hemorrhaging contributed to such a rapid progression of disease. Gerbil models that developed severe pulmonary lesions with rapid disease progression are compared to symptoms in humans known as fulminant pulmonary edema following EV71 infection [3,33]. Severe neurological disorders were also observed in a gerbil model in our previous study [26]. Therefore, gerbil animal models developed both neurological and respiratory clinical features consistent with those observed in humans.

Pulmonary edema is associated with fatal EV71 infection in children [3,4,15,34,35]. Histopathological examination of lung tissue reveals severe pulmonary infiltration and hemorrhagic edema [36,37]. Wu et al. suggested that brainstem lesions and medullar damage could induce autonomic nervous dysfunction, in turn altering pulmonary vascular permeability eventually resulting in pulmonary edema [33]. Chang et al. revealed systemic hypertension and vasoconstriction produced by central sympathetic over activation was responsible for pulmonary edema in humans [3]. While brainstem lesions appeared in cynomolgus monkeys, ICR mice and AG129 mice, no animals developed pulmonary edema. Otherwise, EV71 replication in lungs was boosted at early stages of infection and decreased to a very low level at later time points post-infection in AG129 mice [20,28]. In contrast, EV71 infected gerbil lung tissue and viral replication was persistent, with viral titers reaching $1 \times 10^{5.75}$ TCID₅₀, until they died. We hypothesized that the damage associated with virus replication and the stimulation of inflammatory cytokines in lung tissues is a possible mechanism of pulmonary edema in gerbils. Since the pathogenesis of EV71-induced pulmonary edema and hemorrhage remains unclear, we hypothesized that this gerbil model would provide a useful platform for understanding the pathogenesis of pulmonary edema.

Skeletal muscle has persistent EV71 viral titers and is a vigorous viral source for entry into the blood stream or the CNS, sometimes via peripheral motor nerves [21,38]. These studies suggest IM inoculation of EV71 should be more fatal than IP inoculation, however, we found disease progression to be similar between the two routes in gerbils. In fact, when infected with the same EV71 dose, each inoculation route resulted in death at the same time post infection. Moreover, virus in the muscle tissue was not detected until 3 days p.i. following IP inoculation, suggesting the bloodstream may be the major route of spread in the gerbil model with EV71 spread from muscle to CNS through neuronal pathways constituting a secondary pathway.

Fecal-oral transmission is typically thought to be the main route of EV71 spread, but evidence to support this transmission mode was limited to a few studies [39,40]. ICR pups did not transmit EV71 to their cagemates or dam by clinical isolated EV71 [41], showing this model is not ideal for the study of EV71 infection. EV71 has been isolated in stool specimens and respiratory secretions of EV71 infected children [42], therefore EV71 transmission more than likely occurs by both respiratory and fecal-oral spread. In our preview study, we found EV71 could transmit from infected gerbil to their cagemates on the basis of seroconversion by the field virus strain (data not shown). Here, we demonstrated EV71 could infect gerbils by IM, IP, OL and even by nose route (data not shown). Therefore, EV71 has the ability to infect by multiple routes in a gerbil model, suggesting EV71 infection may transmit by multiple routes in humans. Gerbils may provide an ideal animal model for further investigating various transmission routes infected by EV71. Otherwise, humans are the only known natural host of EV71. Gerbils were so sensitive to EV71 infection and it implied a properly potential reservoir host for EV71 viruses. These findings expanded our view on natural reservoirs of EV71.

Passive immunization fully protected animals from EV71-induced death in newborn mice [41]. Our results here further confirmed the protective role of passive antibodies in EV71 infection in a gerbil model. Kinetic experiments showed that neutralizing antibodies can be detected

at 5–7 days after infection and peak antibody titers appeared at 28 days with the duration of high neutralizing antibody production lasting as long as one month. These results implied that passive immunization against EV71 might be an important alternative therapeutic choice for patients with early EV71 infection.

In conclusion, studies in animal models are essential for understanding the pathophysiology of EV71 and developing therapeutic strategies after EV71 infection. Based on histopathological analysis, our data showed that gerbils can be effectively infected by EV71 and exhibited both neurological and respiratory symptoms in line with those observed in EV71-infected humans. We suggest the gerbil model is the most appropriate model for studying EV71 human disease. EV71-infection induced various pulmonary damage levels in gerbils providing a powerful tool to study the host-pathogen interface of EV71 infection. Finally, the gerbil model can serve as a valuable model for the development of vaccines and therapeutics in future.

Supporting Information

S1 Table. Gerbils were inoculated IP with $1 \times 10^{5.5}$ TCID₅₀ of EV71 at the age of 7 days.
(DOCX)

S2 Table. Gerbils were inoculated IP with $1 \times 10^{5.5}$ TCID₅₀ of EV71 at the age of 14 days.
(DOCX)

S3 Table. Gerbils were inoculated IP with $1 \times 10^{5.5}$ TCID₅₀ of EV71 at the age of 21 days.
(DOCX)

S4 Table. Gerbils were inoculated IP with $1 \times 10^{5.5}$ TCID₅₀ of EV71 at the age of 28 days.
(DOCX)

S5 Table. Gerbils were inoculated IP with $1 \times 10^{5.5}$ TCID₅₀ of EV71 at the age of 35 days.
(DOCX)

S6 Table. 21-day-old gerbils were inoculated with $1 \times 10^{3.5}$ or $1 \times 10^{5.5}$ TCID₅₀ of EV71 via IP.
(DOCX)

S7 Table. 21-day-old gerbils were inoculated with $1 \times 10^{5.5}$ TCID₅₀ of EV71 via IP, IM or OL routes.
(DOCX)

Acknowledgments

The authors thank Professor Xiao Xu for critical review of the manuscript.

Author Contributions

Conceived and designed the experiments: HPZ. Performed the experiments: FX LQ YX PPY ZNY RHX YSS HJL. Analyzed the data: PPY XL YX ZNY RHX YSS ZYZ. Contributed reagents/materials/analysis tools: SCX ZPC JMJ YJZ LLM ZPM CL HG WFL XXH YX ZYX XFF. Wrote the paper: PPY ZNY RHX YSS FX SLL. XX.

References

1. Huang SW, Hsu YW, Smith DJ, Kiang D, Tsai HP, Lin KH, et al. Reemergence of enterovirus 71 in 2008 in taiwan: dynamics of genetic and antigenic evolution from 1998 to 2008. *J Clin Microbiol.* 2009; 47: 3653–3662. doi: [10.1128/JCM.00630-09](https://doi.org/10.1128/JCM.00630-09) PMID: [19776232](https://pubmed.ncbi.nlm.nih.gov/19776232/)

2. Chang LY, Huang YC, Lin TY. Fulminant neurogenic pulmonary oedema with hand, foot, and mouth disease. *Lancet*. 1998; 352: 367–368. PMID: [9717926](#)
3. Chang LY, Lin TY, Hsu KH, Huang YC, Lin KL, Hsueh C, et al. Clinical features and risk factors of pulmonary oedema after enterovirus-71-related hand, foot, and mouth disease. *Lancet*. 1999; 354: 1682–1686. PMID: [10568570](#)
4. Ho M, Chen ER, Hsu KH, Twu SJ, Chen KT, Tsai SF, et al. An epidemic of enterovirus 71 infection in Taiwan. Taiwan Enterovirus Epidemic Working Group. *N Engl J Med*. 1999; 341: 929–935. PMID: [10498487](#)
5. Huang CC, Liu CC, Chang YC, Chen CY, Wang ST, Yeh TF. Neurologic complications in children with enterovirus 71 infection. *N Engl J Med*. 1999; 341: 936–942. PMID: [10498488](#)
6. Zhang D, Lu J. Enterovirus 71 vaccine: close but still far. *Int J Infect Dis*. 2010; 14: e739–743. doi: [10.1016/j.ijid.2009.12.002](#) PMID: [20400350](#)
7. Zeng M, El Khatib NF, Tu S, Ren P, Xu S, Zhu Q, et al. Seroepidemiology of Enterovirus 71 infection prior to the 2011 season in children in Shanghai. *J Clin Virol*. 2012; 53: 285–289. doi: [10.1016/j.jcv.2011.12.025](#) PMID: [22265829](#)
8. Xing W, Liao Q, Viboud C, Zhang J, Sun J, Wu JT, et al. Hand, foot, and mouth disease in China, 2008–12: an epidemiological study. *Lancet Infect Dis*. 2014; 14: 308–318. doi: [10.1016/S1473-3099\(13\)70342-6](#) PMID: [24485991](#)
9. Yang F, Du J, Hu Y, Wang X, Xue Y, Dong J, et al. Enterovirus coinfection during an outbreak of hand, foot, and mouth disease in Shandong, China. *Clin Infect Dis*. 2011; 53: 400–401. doi: [10.1093/cid/cir346](#) PMID: [21785005](#)
10. Yang F, Ren L, Xiong Z, Li J, Xiao Y, Zhao R, et al. Enterovirus 71 outbreak in the People's Republic of China in 2008. *J Clin Microbiol*. 2009; 47: 2351–2352. doi: [10.1128/JCM.00563-09](#) PMID: [19439545](#)
11. Zhang Y, Tan XJ, Wang HY, Yan DM, Zhu SL, Wang DY, et al. An outbreak of hand, foot, and mouth disease associated with subgenotype C4 of human enterovirus 71 in Shandong, China. *J Clin Virol*. 2009; 44: 262–267. doi: [10.1016/j.jcv.2009.02.002](#) PMID: [19269888](#)
12. Jee YM, Cheon DS, Kim K, Cho JH, Chung YS, Lee J, et al. Genetic analysis of the VP1 region of human enterovirus 71 strains isolated in Korea during 2000. *Arch Virol*. 2003; 148: 1735–1746. PMID: [14505086](#)
13. Fujimoto T, Chikahira M, Yoshida S, Ebira H, Hasegawa A, Totsuka A, et al. Outbreak of central nervous system disease associated with hand, foot, and mouth disease in Japan during the summer of 2000: detection and molecular epidemiology of enterovirus 71. *Microbiol Immunol*. 2002; 46: 621–627. PMID: [12437029](#)
14. Chan KP, Goh KT, Chong CY, Teo ES, Lau G, Ling AE. Epidemic hand, foot and mouth disease caused by human enterovirus 71, Singapore. *Emerg Infect Dis*. 2003; 9: 78–85. PMID: [12533285](#)
15. Chan LG, Parashar UD, Lye MS, Ong FG, Zaki SR, Alexander JP, et al. Deaths of children during an outbreak of hand, foot, and mouth disease in sarawak, malaysia: clinical and pathological characteristics of the disease. For the Outbreak Study Group. *Clin Infect Dis*. 2000; 31: 678–683. PMID: [11017815](#)
16. Tu PV, Thao NT, Perera D, Huu TK, Tien NT, Thuong TC, et al. Epidemiologic and virologic investigation of hand, foot, and mouth disease, southern Vietnam, 2005. *Emerg Infect Dis*. 2007; 13: 1733–1741. doi: [10.3201/eid1311.070632](#) PMID: [18217559](#)
17. Xu W, Liu CF, Yan L, Li JJ, Wang LJ, Qi Y, et al. Distribution of enteroviruses in hospitalized children with hand, foot and mouth disease and relationship between pathogens and nervous system complications. *Virology*. 2012; 9: 8. doi: [10.1186/1743-422X-9-8](#) PMID: [22230340](#)
18. Arita M, Ami Y, Wakita T, Shimizu H. Cooperative effect of the attenuation determinants derived from poliovirus sabin 1 strain is essential for attenuation of enterovirus 71 in the NOD/SCID mouse infection model. *J Virol*. 2008; 82: 1787–1797. PMID: [18057246](#)
19. Fujii K, Nagata N, Sato Y, Ong KC, Wong KT, Yamayoshi S, et al. Transgenic mouse model for the study of enterovirus 71 neuropathogenesis. *Proc Natl Acad Sci U S A*. 2013; 110: 14753–14758. doi: [10.1073/pnas.1217563110](#) PMID: [23959904](#)
20. Khong WX, Yan B, Yeo H, Tan EL, Lee JJ, Ng JK, et al. A non-mouse-adapted enterovirus 71 (EV71) strain exhibits neurotropism, causing neurological manifestations in a novel mouse model of EV71 infection. *J Virol*. 2012; 86: 2121–2131. doi: [10.1128/JVI.06103-11](#) PMID: [22130542](#)
21. Chen CS, Yao YC, Lin SC, Lee YP, Wang YF, Wang JR, et al. Retrograde axonal transport: a major transmission route of enterovirus 71 in mice. *J Virol*. 2007; 81: 8996–9003. PMID: [17567704](#)
22. Ong KC, Badmanathan M, Devi S, Leong KL, Cardosa MJ, Wong KT. Pathologic characterization of a murine model of human enterovirus 71 encephalomyelitis. *J Neuropathol Exp Neurol*. 2008; 67: 532–542. doi: [10.1097/NEN.0b013e31817713e7](#) PMID: [18520772](#)

23. Nishimura Y, Shimojima M, Tano Y, Miyamura T, Wakita T, Shimizu H. Human P-selectin glycoprotein ligand-1 is a functional receptor for enterovirus 71. *Nat Med.* 2009; 15: 794–797. doi: [10.1038/nm.1961](https://doi.org/10.1038/nm.1961) PMID: [19543284](https://pubmed.ncbi.nlm.nih.gov/19543284/)
24. Yamayoshi S, Yamashita Y, Li J, Hanagata N, Minowa T, Takemura T, et al. Scavenger receptor B2 is a cellular receptor for enterovirus 71. *Nat Med.* 2009; 15: 798–801. doi: [10.1038/nm.1992](https://doi.org/10.1038/nm.1992) PMID: [19543282](https://pubmed.ncbi.nlm.nih.gov/19543282/)
25. Liu J, Dong W, Quan X, Ma C, Qin C, Zhang L. Transgenic expression of human P-selectin glycoprotein ligand-1 is not sufficient for enterovirus 71 infection in mice. *Arch Virol.* 2012; 157: 539–543. doi: [10.1007/s00705-011-1198-2](https://doi.org/10.1007/s00705-011-1198-2) PMID: [22187102](https://pubmed.ncbi.nlm.nih.gov/22187102/)
26. Yao PP, Qian L, Xia Y, Xu F, Yang ZN, Xie RH, et al. Enterovirus 71-induced neurological disorders in young gerbils, *Meriones unguiculatus*: development and application of a neurological disease model. *PLoS One.* 2012; 7: e51996. doi: [10.1371/journal.pone.0051996](https://doi.org/10.1371/journal.pone.0051996) PMID: [23284845](https://pubmed.ncbi.nlm.nih.gov/23284845/)
27. Reed LJ, Muench H. A simple method of estimating fifty percent endpoints. *AmJHyg.* 1938; 27:493–497.
28. Wang YF, Chou CT, Lei HY, Liu CC, Wang SM, Yan JJ, et al. A mouse-adapted enterovirus 71 strain causes neurological disease in mice after oral infection. *J Virol.* 2004; 78: 7916–7924. PMID: [15254164](https://pubmed.ncbi.nlm.nih.gov/15254164/)
29. Xiu JH, Zhu H, Xu YF, Liu JN, Xia XZ, Zhang LF. Necrotizing myositis causes restrictive hypoventilation in a mouse model for human enterovirus 71 infection. *Virol J.* 2013; 10: 215. doi: [10.1186/1743-422X-10-215](https://doi.org/10.1186/1743-422X-10-215) PMID: [23809248](https://pubmed.ncbi.nlm.nih.gov/23809248/)
30. Lin YW, Yu SL, Shao HY, Lin HY, Liu CC, Hsiao KN, et al. Human SCARB2 transgenic mice as an infectious animal model for enterovirus 71. *PLoS One.* 2013; 8: e57591. doi: [10.1371/journal.pone.0057591](https://doi.org/10.1371/journal.pone.0057591) PMID: [23451246](https://pubmed.ncbi.nlm.nih.gov/23451246/)
31. Nagata N, Iwasaki T, Ami Y, Tano Y, Harashima A, Suzaki Y, et al. Differential localization of neurons susceptible to enterovirus 71 and poliovirus type 1 in the central nervous system of cynomolgus monkeys after intravenous inoculation. *J Gen Virol.* 2004; 85: 2981–2989. PMID: [15448361](https://pubmed.ncbi.nlm.nih.gov/15448361/)
32. Wang YF, Yu CK. Animal models of enterovirus 71 infection: applications and limitations. *J Biomed Sci.* 2014; 21: 31. doi: [10.1186/1423-0127-21-31](https://doi.org/10.1186/1423-0127-21-31) PMID: [24742252](https://pubmed.ncbi.nlm.nih.gov/24742252/)
33. Wu JM, Wang JN, Tsai YC, Liu CC, Huang CC, Chen YJ, et al. Cardiopulmonary manifestations of fulminant enterovirus 71 infection. *Pediatrics.* 2002; 109: E26-. PMID: [11826236](https://pubmed.ncbi.nlm.nih.gov/11826236/)
34. Ho M. Enterovirus 71: the virus, its infections and outbreaks. *J Microbiol Immunol Infect.* 2000; 33: 205–216. PMID: [11269363](https://pubmed.ncbi.nlm.nih.gov/11269363/)
35. Lum LC, Wong KT, Lam SK, Chua KB, Goh AY, Lim WL, et al. Fatal enterovirus 71 encephalomyelitis. *J Pediatr.* 1998; 133: 795–798. PMID: [9842048](https://pubmed.ncbi.nlm.nih.gov/9842048/)
36. Yan JJ, Wang JR, Liu CC, Yang HB, Su IJ. An outbreak of enterovirus 71 infection in Taiwan 1998: a comprehensive pathological, virological, and molecular study on a case of fulminant encephalitis. *J Clin Virol.* 2000; 17: 13–22. PMID: [10814934](https://pubmed.ncbi.nlm.nih.gov/10814934/)
37. Kao SJ, Yang FL, Hsu YH, Chen HI. Mechanism of fulminant pulmonary edema caused by enterovirus 71. *Clin Infect Dis.* 2004; 38: 1784–1788. PMID: [15227628](https://pubmed.ncbi.nlm.nih.gov/15227628/)
38. Manki A, Oda M, Seino Y. Neurologic diseases of enterovirus infections: polioviruses, coxsackieviruses, echoviruses, and enteroviruses type 68–72. *Nihon Rinsho.* 1997; 55: 849–854. PMID: [9434576](https://pubmed.ncbi.nlm.nih.gov/9434576/)
39. Chang LY, King CC, Hsu KH, Ning HC, Tsao KC, Li CC, et al. Risk factors of enterovirus 71 infection and associated hand, foot, and mouth disease/herpangina in children during an epidemic in Taiwan. *Pediatrics.* 2002; 109: e88. PMID: [12042582](https://pubmed.ncbi.nlm.nih.gov/12042582/)
40. Chang LY, Tsao KC, Hsia SH, Shih SR, Huang CG, Chan WK, et al. Transmission and clinical features of enterovirus 71 infections in household contacts in Taiwan. *JAMA.* 2004; 291: 222–227. PMID: [14722149](https://pubmed.ncbi.nlm.nih.gov/14722149/)
41. Yu CK, Chen CC, Chen CL, Wang JR, Liu CC, Yan JJ, et al. Neutralizing antibody provided protection against enterovirus type 71 lethal challenge in neonatal mice. *J Biomed Sci.* 2000; 7: 523–528. PMID: [11060501](https://pubmed.ncbi.nlm.nih.gov/11060501/)
42. Pallansch M, Roos R. Enteroviruses: polioviruses, coxsackieviruses, echoviruses, and newer enteroviruses. In: Knipe DM, Howley PM, eds. *Fields' Virology.* 5th ed. Philadelphia, PA: Lippincott, Williams and Wilkins; 2007: pp840–894.